



Published in final edited form as:

J Urol. 2016 July ; 196(1): 270–278. doi:10.1016/j.juro.2015.12.081.

Fetal rat gubernaculum mesenchymal cells adopt myogenic and myofibroblast-like phenotypes

Alan K. Robbins^{1, #}, Abigail B. Mateson^{1, #}, Ashutosh Khandha⁴, Joan E. Pugarelli¹, Thomas S. Buchanan^{3, 4}, Robert E. Akins^{2, 4}, and Julia Spencer Barthold¹

¹Pediatric Urology Research Laboratory, Nemours Biomedical Research/Alfred I. duPont Hospital for Children, Wilmington, DE

²Tissue Engineering and Regenerative Medicine Research Laboratory, Nemours Biomedical Research/Alfred I. duPont Hospital for Children, Wilmington, DE

³Department of Mechanical Engineering, University of Delaware, Newark, DE

⁴Department of Biomedical Engineering, University of Delaware, Newark, DE

Abstract

Purpose—Gubernaculum-cremaster complex (GCC) development is hormonally-regulated and abnormal in a cryptorchid rat model. Using cell tracking techniques and imaging, we studied myogenic phenotypes and fates in the fetal rat GCC.

Materials and methods—E17 (embryonic day 17) GCCs were labeled with CellTracker™ or DNA synthesis marker 5-ethynyl-2'-deoxyuridine (EdU), or immobilized in Matrigel™ and grown in culture. E17-21 GCC sections and cells were imaged using widefield and deconvolution immunofluorescence microscopy and muscle- and/or myofibroblast-specific antibodies. Deconvolved image stacks were used to create a 3-dimensional (3D) model of E21 GCC muscle.

Results—Paired-box 7 (PAX7)⁺ and myogenin⁺ muscle precursors were visible in a desmin-rich “myogenic zone” between muscle layers that elongated and became thicker during development. GCC inner mesenchymal cells expressed desmin and alpha smooth muscle actin (α SMA) at lower levels than in the myogenic zone. After pulse-labeling with CellTracker™ or EdU, mesenchymal cells became incorporated into differentiated muscle. Conversely, mesenchymal cells migrated beyond Matrigel™-immobilized GCCs, expressed PAX7 and fused to form striated myotubes. Mesenchymal GCC cell lines proliferated >40 passages and exhibited contractile behavior, but did not form striated muscle. Our 3D GCC model showed 2 orthogonal ventral layers and an arcing inner layer of muscle.

Conclusions—Our data suggest that mesenchymal cells in the peripheral myogenic zone of the fetal GCC contribute to formation of a distinctively-patterned cremaster muscle. Non-

Correspondence to: Julia S. Barthold, Nemours Biomedical Research/Alfred I. duPont Hospital for Children, 1701 Rockland Rd., Wilmington DE 19803; Julia.Barthold@nemours.org.

[#]These authors contributed equally to this work

Publisher's Disclaimer: This is a PDF file of an unedited manuscript that has been accepted for publication. As a service to our customers we are providing this early version of the manuscript. The manuscript will undergo copyediting, typesetting, and review of the resulting proof before it is published in its final citable form. Please note that during the production process errors may be discovered which could affect the content, and all legal disclaimers that apply to the journal pertain.

myogenic, desmin- and α SMA-positive GCC mesenchymal cells proliferate and exhibit a myofibroblast-like phenotype in culture. Intrinsic mechanical properties of these divergent cell types may facilitate perinatal inversion of the GCC.

Keywords

gubernaculum; muscle; myofibroblasts; rat strains; computer modeling

INTRODUCTION

The gubernaculum directs fetal testicular descent via swelling and migration.^{1,2} Failed descent leads to cryptorchidism (undescended testis, UDT), a common anomaly in boys.³ The fetal cremaster develops at the periphery of the mesenchymal gubernacular cone in rats, and the resultant gubernaculum-cremaster complex (GCC) inverts around the time of birth. In humans, the cremaster develops both within and around the gubernacular mesenchyme,⁴ but the basic development of the GCC is similar among mammals.^{1,2}

GCC development requires activation of the androgen receptor (AR) by androgens and of the relaxin insulin-like family peptide receptor 2 (RXFP2) by insulin-like 3 (INSL3). In the fetal rat, there is strong overlap in the transcriptional response of the GCC to these hormones,⁵ but their common and unique effects at the cellular level remain incompletely defined. Both hormones are required for enlargement and patterning of the cremaster muscle.^{6,7} Transgenic inactivation of *Rxfp2* leads to complete disorganization, lack of swelling and absent muscle development, in contrast to *Ar* inactivation targeting mesenchymal cells, which results in more subtle muscle defects. Similarly, *Rxfp2* expression in the GCC is diffuse at E14,⁸ but the RXFP2 protein becomes localized to the muscle layer by E20.5.⁹ Beta-catenin (CTNNB), Notch and Wilm's tumor 1 (WT1) are also required for myogenic differentiation of the GCC.^{6,10} Moreover, altered expression of muscle-specific genes and focally defective muscle development occur in the fetal GCC of the congenitally cryptorchid LE/orl rat.^{11,12}

The origin of developing cremaster muscle fibers and the factor(s) triggering GCC inversion remain incompletely understood and/or controversial.^{4,13,14} We studied myogenic marker expression in fetal tissues and used in vitro models to study development of GCC muscle. Our data suggest that certain GCC mesenchymal cells are myogenic precursors that differentiate into striated muscle and contribute to formation of a distinctively patterned cremaster, while others adopt a myofibroblast-like phenotype that may contribute to generation of tonic force within the GCC.

MATERIALS AND METHODS

Animals

Long Evans rats (Charles River Laboratories) aged 2–3 months were maintained at the Nemours Biomedical Research facility (accredited by the Association for Assessment and Accreditation of Laboratory Animal Care International), and animal care and use was approved by the Institutional Animal Care and Use Committee. Care was provided, timed

pregnancies generated and euthanasia performed as described previously;¹² the morning of the day of sperm detection was designated embryonic day 0 (E0).

GCC harvest for imaging and organ culture

GCC pairs were removed as pelvic blocks at E17, 19, and 21, fixed in 4% paraformaldehyde (PFA) in 1x phosphate buffered saline (PBS, pH 7.4), incubated in 28% sucrose at +4°C, embedded in Tissue-Tek O.C.T. compound (VW R) and stored at -70°C as described previously.¹² For organ culture, individual E17 GCCs were placed into 6-well tissue culture dishes coated with poly-L lysine (PLL) 0.01% (70–150 kDa, Sigma) and mouse laminin 8µg/ml (EMD Millipore), and immobilized in Matrigel™ Membrane Matrix 8.5mg/ml (Corning) with warming at 37°C for 10 minutes. We maintained organ cultures in growth medium (Dulbecco's Modified Eagle Medium/Nutrient Mixture F-12 (DMEM/F12), 10% fetal calf serum (FCS) and penicillin-streptomycin (pen-strep); all from ThermoFisher Scientific) in a humidified incubator at 37°C with 5% CO₂. We incubated intact E17 GCCs with CellTracker™ green 5-chloromethylfluorescein diacetate dye (10µM for 5, 10 or 20min) or Click-iT® EdU (5-ethynyl-2'-deoxyuridine for 10min, both from ThermoFisher Scientific) to label peripheral mesenchymal and replicating cells, respectively. GCC blocks were washed 4 times with DMEM/F12, and fixed in 4% PFA/PBS immediately on ice (controls) or placed in culture on Millicell® inserts (EMD Millipore) in 6-well plates with DMEM/F12, 10% FCS and pen-strep for 24h. All tissues were fixed for 45min on ice in 4% PFA/PBS, incubated in 0.1% Triton X100 (Sigma) in PBS on ice, gently washed twice with PBS and stored at +4°C in PBS containing 0.05% sodium azide until embedding. Experiments were repeated at least 3 times with samples from different litters.

GCC cell lines

E17 GCCs were incubated overnight with 5mg/ml collagenase (Worthington) in Hanks' Balanced Salt Solution (HBSS, pH6.7–7.8, Gibco) supplemented with 3mM CaCl₂ at 4°C. The organs were triturated and cells plated onto collagen I-coated T25 flasks (Corning) in selective medium (Medium A) adapted from conditional cell immortalization studies,¹⁵ and consisting of DMEM/F12, pen-strep, 18% FCS, rat epidermal growth factor, 10ng/ml (EGF; Peprotech), rat basic fibroblast growth factor, 1ng/ml (bFGF; Peprotech), bovine insulin, 5µg/ml (Gemini), dexamethasone, 0.4µg/ml (Sigma), cholera toxin, 8.4ng/ml (EMD Millipore), 2-mercaptoethanol, 10µM (Sigma) and the rho kinase inhibitor Y27632, 10nM (Tocris). Cells were maintained in a humidified incubator at 37°C with 5% CO₂ and following initial growth, frozen in cell freezing medium (ScienCell CFM) and stored in liquid nitrogen. Cells were passaged using trypsin 0.25%/EDTA (ThermoFisher Scientific), stained with trypan blue (Sigma) to determine viability, counted using a hemocytometer, and plated at defined densities on collagen I-coated tissue culture plates for further passaging and growth analysis. For isolation of primary cells we used Medium B: DMEM/F12, EGF, bFGF and dexamethasone at the same concentrations noted above.

In vitro GCC cellular phenotype

We seeded GCC cells (passage 5; 5X10⁻⁴ cells per well) on collagen I-coated plates in Medium A to study myogenic differentiation in vitro. After growth of cells to approximately 90% confluence, the medium was replaced with Medium A without Y27632. After 72h

without Y27632, low serum medium was added (DMEM/F12, pen-strep, ITS (insulin/transferrin/selenium) and 2% FCS) and cells grown for an additional 5-7 days with phase-contrast documentation of cell morphology daily and medium changes every other day.

Immunofluorescent (IF) imaging of GCC sections and cell cultures

We used IF to localize muscle differentiation markers myogenin and myosin heavy chain (MyHC); desmin, a myoid marker that is expressed early in myogenic differentiation, in differentiated muscle, and in some myofibroblast cell subtypes;^{16,17} smooth muscle alpha actin (α SMA), expressed during development of fetal striated muscle¹⁸ and in myofibroblasts;¹⁹ and paired-box 7 (PAX7) and integrin alpha 7 (ITGA7), markers more highly expressed in fetal as compared to embryonic myoblasts.^{20,21} Details of the primary antibodies used are shown in Table 1. Sections (10 μ m) were obtained using a Leica CM3050 cryostat, and collected on SuperFrost Plus slides (Fisher). Slides were treated with 0.1% Triton X100 in PBS, incubated in 3% bovine serum albumin (BSA)/PBS solution for 1h at room temperature and then overnight at +4°C with primary antibodies in PBS. After washing 3 times with PBS, slides were incubated with Alexa Fluor secondary antibodies (ThermoFisher Scientific) in PBS for 1h, counterstained with 4',6-diamidino-2-phenylindole (DAPI) and mounted in IF medium (Dako). We also imaged passage 1 (P1) cells plated at low density (5×10^4) in Medium B and grown for 24h, then fixed and processed as described above. Negative control sections for each experiment were stained with secondary antibody only.

Computer modeling of GCC muscle

E21 GCCs were immunostained with anti-myosin heavy chain antibody (MyHC, all isoforms; A4.1025, Developmental Studies Hybridoma Bank) after optical clearing using the benzyl alcohol/benzyl benzoate (BABB) protocol as described previously.¹² We created image sets, overlapping as needed, to include the entire organ to its point of attachment at the abdominal wall. Z-stack sagittal images were acquired and deconvolved using AutoQuant[®] software (Media Cybernetics). We used a longitudinal muscle gap to orient samples based on our observation that it consistently faces the midline. Selected deconvolved image stacks were modeled to show muscle fiber patterns in a three dimensional (3D) reconstruction using ScanIP[®] (Simpleware Ltd).

RESULTS

Myogenesis proceeds from proximal to distal and superficial to deep within the GCC

As expected, desmin-specific IF of E17-E21 sections showed bright labeling of differentiated skeletal muscle (Figure 1). In the E17 GCC, we observed a thin outer layer and a developing inner layer extending from the abdominal wall to the midportion of the organ, a lack of muscle at the distal tip. At later time points, the 2 layers became progressively thicker and more apposed (Figure 1C–D). In addition, mesenchymal cells throughout the GCC expressed desmin, with staining more intense between the 2 muscle layers, at the distal tip, and within mesothelial cells that cover the GCC. The desmin-rich region between muscle layers suggests enrichment of potential myogenic precursors.

GCC mesenchymal cells proliferate, express PAX7 and myogenin, and are incorporated into developing muscle

Strong immunoreactivity for myogenin and PAX7 was present within muscle nuclei, as expected, but also present in a subset of non-muscle cells in the myogenic zone between muscle layers at E17-19 (Figures 2A–B and 4A–B). Like desmin, α SMA is expressed at high levels in fetal muscle,¹⁸ but is also present in adjacent, non-skeletal muscle cells and within the central core of the GCC (Figure 2). Using platelet endothelial cell adhesion molecule (PECAM/CD31) IF to define vascular endothelial cells, we confirmed that non-vascular, mesenchymal cells also express α SMA, but at lower levels than in the differentiated muscle (Figure 3). Centrally-located mesenchymal cells also expressed desmin at lower levels than present in the peripheral myogenic zone (Figures 1 and 4).

In experiments designed to track the fate of peripheral mesenchymal (mesothelial) cells in E17 organ cultures, we used CellTracker™ dye, which diffuses into cells but is not transferred across cell membranes, and Click-it® EdU, which is incorporated into DNA of replicating cells. In preliminary experiments designed to limit CellTracker™ labeling to mesothelial cells, we found that exposure of GCCs for 10min allowed the dye to penetrate into the existing muscle layer, but a shorter exposure time (5min) pulse labeled only mesothelial cells in control samples (Figure 5A) and was used in subsequent experiments. After 24h of culture, we found that CellTracker™-labelled cells or their progeny formed multiple superficial layers, had penetrated deep to the muscle layer, and overlapped with MyHC staining within the muscle (Figure 5B). These data suggest that GCC mesothelial cells proliferate, and via incorporation and/or migration, contribute to developing layers of muscle. CellTracker™ dye can passively enter existing myotubes, so we also labeled E17 GCCs by brief exposure to EdU to define the fate of proliferating (non-muscle) cells. EdU was successfully incorporated into mesenchymal cell nuclei within the myogenic zone after pulse labeling (Supplementary Figure 1A). After 24h, proliferating cells were visible throughout the GCC and occasional labeled nuclei were present within differentiated myotubes (Supplementary Figure 1B), suggesting that some GCC mesenchymal cells are myogenic precursors and contribute to cellular accretion in the developing cremaster.

GCC myogenic precursors migrate and differentiate into striated muscle in organ culture

During culture of whole GCCs immobilized in Matrigel™, we observed progressive, outward migration of cells away from the mesothelial and cut surfaces of the organ over 3–5 days (Figure 6A). Migrating cells exhibited an unusual, anastomosing architecture comprising elongated spindle cells (Figure 6B). We observed general desmin and α SMA expression, and myogenin and PAX7 expression in some migrating cells (Figure 6C–D). All cells expressed ITGA7, and some cells fused to form multinucleated, striated, MyHC-positive myotubes (Figure 6E). These data suggest that GCC mesenchymal cells can undergo myogenic differentiation under favorable conditions.

GCC cell lines adopt a myofibroblast-like phenotype

We used the Rho kinase inhibitor Y27632 to generate “conditionally immortalized” GCC cell lines that showed continuous proliferation without loss of viability after >40 passages. Cells grown on collagen-coated plates in Medium A exhibited 2 distinct morphologies:

spindle-like cells with elongated processes and low cytoplasmic volumes and flattened cells (Supplementary Figure 2A). Without Y27632, these primary cells became senescent after 4–5 passages. IF imaging of early (0–3) passage cells using a range of muscle markers (Supplementary Figure 2B–D) showed expression of desmin, ITGA7, and myogenin, but PAX7, α SMA, and MyHC were absent, suggesting that all were potentially myogenic but not fully differentiated. However, when we attempted to stimulate myogenesis in subconfluent cultures by removing growth factors and switching to low serum medium, we did not observe significant MyHC expression or myotube formation. Instead, we observed alignment of cells, gradual formation of cleared areas (Figure 7A) and formation of 3D cellular ridges (Figure 7B), most likely due to localized cellular contraction. We also noted that mechanical disturbance of the monolayer with a Pasteur pipet produced rapid release of cells from the plate, behavior suggestive of mechanical tension within the cell layer, which is characteristic of myofibroblasts.

Distinctive muscle patterning of the rat GCC

We generated a 3D GCC model based on MyHC staining of optically cleared E21 samples. In this model, the deeper cremaster muscle layer is continuous and arcs inferomedially, and a ventral, transverse superficial layer creates an orthogonal pattern (Supplementary Figure 3). Both layers were discontinuous medially and at the distal GCC tip, forming a cylindrical structure that was reminiscent of the “strip-like” architecture present in large mammals.¹

DISCUSSION

Myogenesis appears to be an important component of GCC development, suggesting that muscle-generated mechanical force is required for gubernacular function.² However, the means by which internal or external forces trigger GCC migration/inversion are not clear. In animal models of UDT, including deleted *Ar*, *Wt1*, *Insl3*, *Rxfp2*, *Ctnnb*, and *Notch1* transgenic mice, fetal cremaster muscle development is absent, impaired, or disorganized.^{6,7,10,14} The cremaster is more prominent in rodents, but imaging studies show embedded cremaster muscle bundles within human fetal gubernaculum.⁴ Hutson and colleagues have focused primarily on the properties of the GCC that promote its elongation once inversion is complete.² They reported that cremaster differentiation continues after birth, and contributes to final descent of the testis via direct or indirect AR signaling, and to spontaneous contraction of the postnatal GCC.² We observed that prenatal muscle development is abnormal in the GCC of the cryptorchid LE/orl rat, and although inversion occurs, the GCC is subsequently diverted into the superficial inguinal pouch postnatally.¹² We were, thus, motivated to perform additional prenatal studies to define the cellular properties of the rat GCC that set the stage for normal inversion.

Our data suggest that fetal GCC mesenchymal cells differentiate into muscle within a desmin-enriched myogenic zone, a region also evident in prior imaging studies²² and enriched for expression of proteins encoded by candidate genes for cryptorchidism susceptibility in the LE/orl rat.²³ We observed strong nuclear expression of PAX7 and/or myogenin in scattered mesenchymal cells between muscle layers. EdU labeling showed that proliferation is robust in the myogenic zone, and many EdU+ cells also express PAX7, as

shown previously in studies of striated muscle myogenesis.²⁴ CellTracker™+ mesothelial cells and EdU+ non-muscle cells became incorporated into cremaster muscle of cultured GCCs. GCC mesothelial cells are prominent,²⁵ and express WT1 in the E13.5 mouse¹⁰ and E17 rat (Barthold et al, unpublished). Notably, cell fate mapping of WT1-expressing or lipophilic dye-labeled mesothelial cells show similar internal migration²⁶ and contribute to vascular smooth muscle and mesenchyme, including myofibroblasts, within lung and abdominal organs.^{26,27}

In complementary cell fate experiments, we cultured untreated GCCs on Matrigel™ and observed progressive outward migration of mesenchymal cells, with a subset expressing PAX7 and/or myogenin, and multinucleated myotube formation. Since differentiated muscle fibers are non-migratory, these data also suggest that GCC mesenchymal cells can undergo myogenic differentiation. In contrast, when generating GCC cell lines, we found that once dissociated, these cells do not show commitment to myogenesis, as they do not express PAX7 or undergo myogenic differentiation in vitro. This may suggest a requirement for paracrine signaling from existing muscle to promote survival of PAX7+ progenitors.²⁰

Despite evidence that GCC mesenchymal cells are able to form muscle, many do not, although they may express myoid markers such as desmin, myogenin, ITGA7 and α SMA. Interestingly, Barteczko also identified α SMA-expressing mesenchyme in sections of human fetal gubernaculum⁴ and interpreted this finding as evidence for smooth muscle, although other cells, such as myofibroblasts, express this protein. Myofibroblasts produce extracellular matrix (ECM), a major feature of GCC swelling in larger mammals, and may express myogenic markers, such as desmin and myogenin.¹⁹ In developing our GCC cell lines, we likely selected for cells exhibiting morphology and contractile behavior remarkably similar to cell lines originating from similar tissues, including so-called “fibroblast and smooth muscle cells” (FSMCs) and pericytes (myogenic or myofibroblastic cells), derived from mesothelial and differentiated muscle tissues, respectively.^{28,29} Similarly, prostate stromal cells and peritubular myoid cells are α SMA+, express AR, and exhibit contractile behavior in culture.³⁰ While our culture conditions may not fully recapitulate conditions in vivo, they support the possibility that GCC mesenchymal cells can function as myofibroblasts.

Using 3D imaging of E21 GCCs after myosin immunostaining and tissue clearing, we confirmed an unusual arcing pattern of cremaster fiber development that creates a spiral-like organization, differs significantly from the established model of a simple, sac-like rodent GCC¹ and confirms prior published data showing that muscle is absent at the tip of the organ.^{2,12} The medial discontinuity of muscle suggests greater similarity to the “strip-like” cremaster of larger mammals, as noted previously.² We found transverse muscle defects in LE/orl rat GCCs,¹² suggesting that focal defects within this shawl-like muscle may predispose to GCC malfunction and UDT. The importance of muscle contraction in prenatal migration of the mammalian gubernaculum remains controversial.⁴ However, our data suggesting that mesenchymal cells with the ability to generate tonic contractile forces exist within the GCC raises the possibility that they may contribute to the downward force necessary for inversion and testicular descent.

In summary, these data provide further insight into muscle development within the rat GCC and suggest that local mesenchymal precursors contribute to formation of a highly patterned cremaster muscle during late gestation. Expression of α SMA and desmin in mesenchymal cells of the GCC, and propagation of GCC-derived cells that exhibit a contractile phenotype, suggest that myofibroblast differentiation also occurs in the GCC and may contribute to its motility. The phenomena that we observed in our in vitro models occurred without androgen supplementation of serum-containing medium, so further studies will be required to address the role of AR in muscle and myofibroblast differentiation. In future work, we will also use these developmental models to study the functional effects of UDT genetic susceptibility alleles on cell type-specific differentiation of the fetal GCC, using the cryptorchid LE/orl rat strain. With improved understanding of the topology and regulation of GCC muscle and myofibroblast development, we will be able to generate hypotheses that address how these cell types contribute to the mechanical properties of the GCC.

Supplementary Material

Refer to Web version on PubMed Central for supplementary material.

Acknowledgments

Funding: This work was supported by R01HD060769, the *Eunice Kennedy Shriver* National Institute for Child Health and Human Development (NICHD), P20GM103464 from the National Institute of General Medical Sciences (NIGMS), R01HL108110 from the National Heart Lung and Blood Institute, and Nemours Biomedical Research.

Key to abbreviations

UDT	undescended testis
GCC	gubernaculum-cremaster complex
EdU	5-ethynyl-2'-deoxyuridine
PFA	paraformaldehyde
PBS	phosphate-buffered saline
3D	3-dimensional
MyHC	myosin heavy chain
αSMA	smooth muscle alpha actin
PAX7	paired box 7
ITGA7	integrin alpha 7

References

1. Amann RP, Veeramachaneni DN. Cryptorchidism in common eutherian mammals. *Reproduction*. 2007; 133:541. [PubMed: 17379650]

2. Lie G, Hutson JM. The role of cremaster muscle in testicular descent in humans and animal models. *Pediatr Surg Int.* 2011; 27:1255. [PubMed: 22038274]
3. Kollin C, Ritzen EM. Cryptorchidism: a clinical perspective. *Pediatr Endocrinol Rev.* 2014; 11:240. [PubMed: 24683948]
4. Barteczko KJ, Jacob MI. The testicular descent in human. Origin, development and fate of the gubernaculum Hunteri, processus vaginalis peritonei, and gonadal ligaments. *Adv Anat Embryol Cell Biol.* 2000; 156:1.
5. Barthold JS, Wang Y, Robbins A, et al. Transcriptome analysis of the dihydrotestosterone-exposed fetal rat gubernaculum identifies common androgen and insulin-like 3 targets. *Biol Reprod.* 2013; 89:143. [PubMed: 24174575]
6. Kaftanovskaya EM, Feng S, Huang Z, et al. Suppression of insulin-like3 receptor reveals the role of beta-catenin and Notch signaling in gubernaculum development. *Mol Endocrinol.* 2011; 25:170. [PubMed: 21147849]
7. Kaftanovskaya EM, Huang Z, Barbara AM, et al. Cryptorchidism in mice with an androgen receptor ablation in gubernaculum testis. *Mol Endocrinol.* 2012; 26:598. [PubMed: 22322597]
8. Scott DJ, Fu P, Shen PJ, et al. Characterization of the rat INSL3 receptor. *Annals of the New York Academy of Sciences.* 2005; 1041:13. [PubMed: 15956681]
9. McKinnell C, Sharpe RM, Mahood K, et al. Expression of insulin-like factor 3 protein in the rat testis during fetal and postnatal development and in relation to cryptorchidism induced by in utero exposure to di (n-Butyl) phthalate. *Endocrinology.* 2005; 146:4536. [PubMed: 16037377]
10. Kaftanovskaya EM, Neukirchner G, Huff V, Agoulnik AI. Left-sided cryptorchidism in mice with Wilms' tumour 1 gene deletion in gubernaculum testis. *J Pathol.* 2013; 230:39. [PubMed: 23288785]
11. Barthold JS, McCahan SM, Singh AV, et al. Altered expression of muscle- and cytoskeleton-related genes in a rat strain with inherited cryptorchidism. *J Androl.* 2008; 29:352. [PubMed: 18222913]
12. Barthold JS, Robbins A, Wang Y, et al. Cryptorchidism in the orl rat is associated with muscle patterning defects in the fetal gubernaculum and altered hormonal signaling. *Biol Reprod.* 2014; 91:41. [PubMed: 24966393]
13. Radhakrishnan J, Morikawa Y, Donahoe PK, Hendren WH. Observations on the gubernaculum during descent of the testis. *Invest Urol.* 1979; 16:365. [PubMed: 34579]
14. Zimmermann S, Steding G, Emmen JM, et al. Targeted disruption of the *Insl3* gene causes bilateral cryptorchidism. *Mol Endocrinol.* 1999; 13:681. [PubMed: 10319319]
15. Chapman S, Liu X, Meyers C, Schlegel R, McBride AA. Human keratinocytes are efficiently immortalized by a Rho kinase inhibitor. *J Clin Invest.* 2010; 120:2619. [PubMed: 20516646]
16. Schmitt-Graff A, Desmouliere A, Gabbiani G. Heterogeneity of myofibroblast phenotypic features: an example of fibroblastic cell plasticity. *Virchows Arch.* 1994; 425:3. [PubMed: 7921410]
17. Capetanaki Y, Milner DJ, Weitzer G. Desmin in muscle formation and maintenance: knockouts and consequences. *Cell Struct Funct.* 1997; 22:103. [PubMed: 9113396]
18. Babai F, Musevi-Aghdam J, Schurch W, Royal A, Gabbiani G. Coexpression of alpha-sarcomeric actin, alpha-smooth muscle actin and desmin during myogenesis in rat and mouse embryos I. Skeletal muscle. *Differentiation.* 1990; 44:132. [PubMed: 2283002]
19. Walker GA, Guerrero IA, Leinwand LA. Myofibroblasts: molecular crossdressers. *Curr Top Dev Biol.* 2001; 51:91. [PubMed: 11236717]
20. Kassari-Duchossoy L, Giaccone E, Gayraud-Morel B, Jory A, Gomes D, Tajbakhsh S. Pax3/Pax7 mark a novel population of primitive myogenic cells during development. *Genes Dev.* 2005; 19:1426. [PubMed: 15964993]
21. Biressi S, Tagliafico E, Lamorte G, et al. Intrinsic phenotypic diversity of embryonic and fetal myoblasts is revealed by genome-wide gene expression analysis on purified cells. *Dev Biol.* 2007; 304:633. [PubMed: 17292343]
22. Nation TR, Buraundi S, Farmer PJ, et al. Development of the gubernaculum during testicular descent in the rat. *Anat Rec (Hoboken).* 2011; 294:1249. [PubMed: 21618435]
23. Barthold JS, Pugarelli J, MacDonald ML, et al. Polygenic inheritance of cryptorchidism susceptibility in the LE/orl rat. *Mol Hum Reprod.* 2015 in press.

24. Esteves de Lima J, Bonnin MA, Bourgeois A, Parisi A, Le Grand F, Duprez D. Specific pattern of cell cycle during limb fetal myogenesis. *Dev Biol.* 2014; 392:308. [PubMed: 24882711]
25. Buraundi S, Balic A, Farmer PJ, Southwell BR, Hutson JM. Gubernacular development in the mouse is similar to the rat and suggests that the processus vaginalis is derived from the urogenital ridge and is different from the parietal peritoneum. *J Pediatr Surg.* 2011; 46:1804. [PubMed: 21929994]
26. Que J, Wilm B, Hasegawa H, Wang F, Bader D, Hogan BL. Mesothelium contributes to vascular smooth muscle and mesenchyme during lung development. *Proc Natl Acad Sci U S A.* 2008; 105:16626. [PubMed: 18922767]
27. Batra H, Antony VB. The pleural mesothelium in development and disease. *Front Physiol.* 2014; 5:284. [PubMed: 25136318]
28. Cappellari O, Cossu G. Pericytes in development and pathology of skeletal muscle. *Circ Res.* 2013; 113:341. [PubMed: 23868830]
29. Rinkevich Y, Mori T, Sahoo D, Xu PX, Bermingham JR Jr, Weissman IL. Identification and prospective isolation of a mesothelial precursor lineage giving rise to smooth muscle cells and fibroblasts for mammalian internal organs, and their vasculature. *Nat Cell Biol.* 2012; 14:1251. [PubMed: 23143399]
30. Swinnen K, Deboel L, Cailleau J, Heyns W, Verhoeven G. Morphological and functional similarities between cultured prostatic stromal cells and testicular peritubular myoid cells. *Prostate.* 1991; 19:99. [PubMed: 1656413]

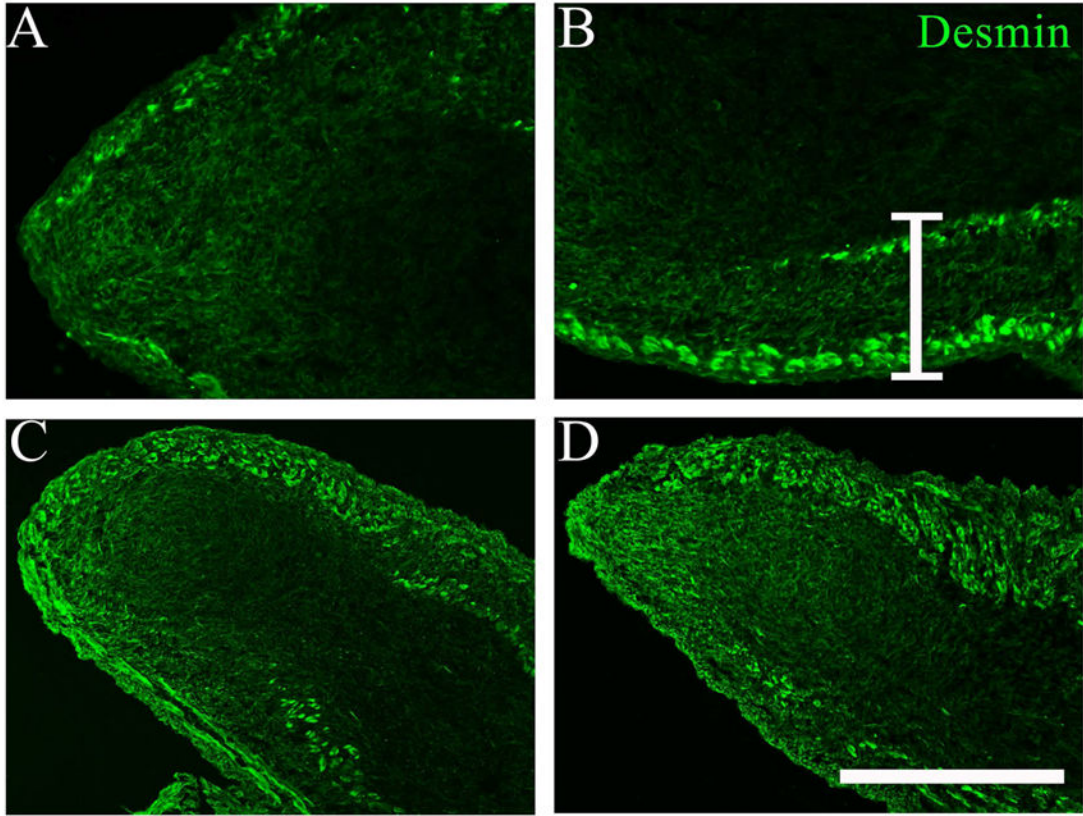


Figure 1.

Immunostaining of E17 (embryonic day 17; A, B); E19 (C) and E21 (D) rat gubernaculum-cremaster complex (GCC) sections for desmin (green); the distal GCC is on the left and the more proximal GCC on the right side of each frame. Differentiated muscle layers stain brightly for desmin in each image. A. A single, thin peripheral muscle layer is visible at E17 with an opening present at the GCC tip (left); desmin expression is much lower in the central mesenchymal core, but enriched at the tip. B. A more proximal image from the same section shows a second, inner muscle layer developing in the proximal half of the GCC, and enrichment of desmin-positive mesenchymal cells between the muscle layers, an apparent “myogenic zone”, indicated by the white bracket. C. Thickening of both muscle layers is visible at E19. D. Further development by E21 has obliterated the space between muscle layers in this view (top). A,B: scale bar=200 μm ; C,D: scale bar=400 μm .

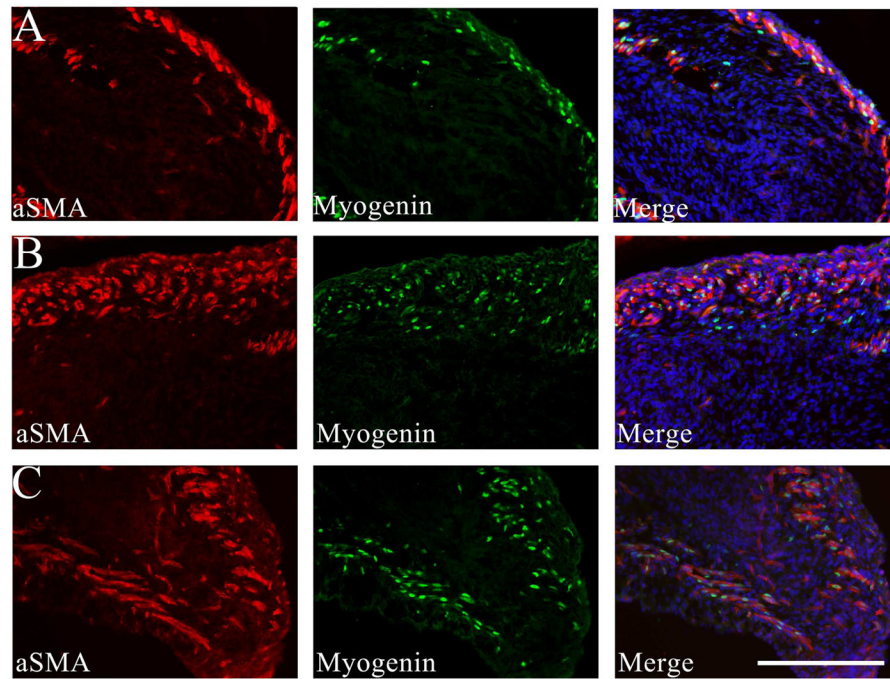


Figure 2.

Immunostaining of E17 (A), E19 (B) and E21 (C) GCC sections for alpha smooth muscle actin (α SMA; red) and myogenin (green); the distal GCC is on the right and the more proximal GCC on the left side of each frame. Differentiated muscle layers stain brightly for α SMA in each image, and DAPI counterstaining in the merged image shows the position of the inner mesenchyme relative to muscle layers. A. At E17, cells with nuclear myogenin staining are primarily within, but occasionally between, the differentiated muscle layers. B. At E19, additional myogenin-positive cells are visible between the developing muscle layers (right) that define the “myogenic zone”. Scale bar=200 μ m. Sections are adjacent to those shown in Figure 4.

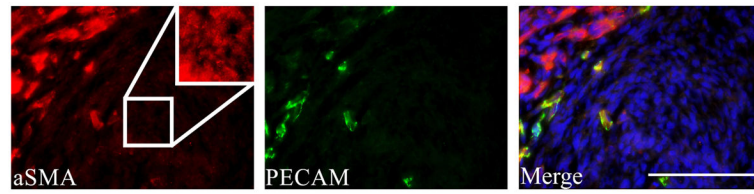


Figure 3. Immunostaining of E19 GCC sections for (A) alpha smooth muscle actin (α SMA; red) and (B) platelet endothelial cell adhesion molecule (PECAM/CD31; green) shows strong expression of α SMA within differentiated muscle (left upper corner of image), and fainter mesenchymal expression within the GCC core (right lower corner of image). Coexpression of α SMA and PECAM in blood vessels appears yellow in merged image. A PECAM-negative region within the core is magnified and enhanced (inset) for better visualization of mesenchymal α SMA. Scale bar=100 μ m.

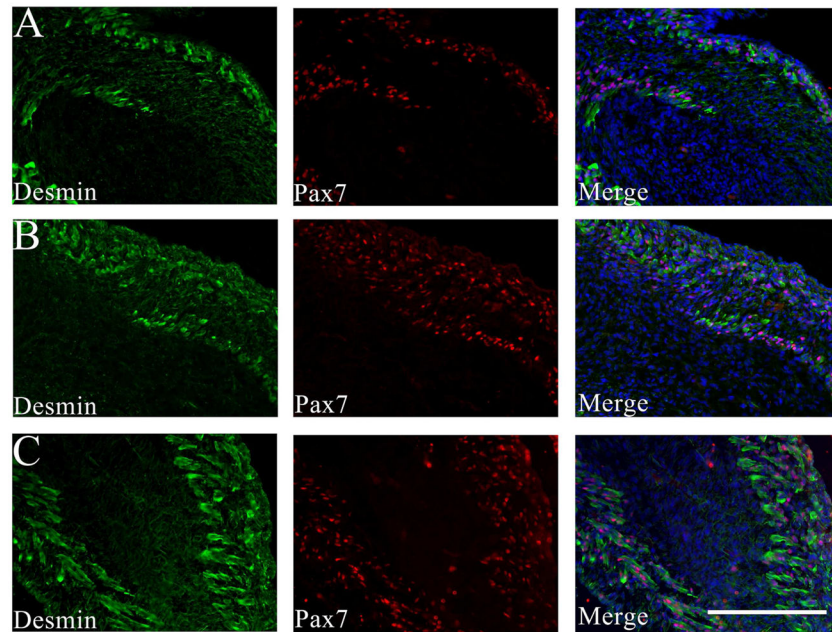


Figure 4. Immunostaining of E17 (A), E19 (B), and E21 (C) GCC sections for desmin (green) and paired box 7 (PAX7, red); the distal GCC is on the right and the more proximal GCC on the left side of each frame. Differentiated muscle layers stain brightly for desmin in each image, and DAPI counterstaining in the merged image shows the position of the inner mesenchyme relative to muscle layers. A. At E17, cells with nuclear PAX7 staining are primarily within, but occasionally between, the differentiated muscle layers. B. At E19, additional PAX7-positive cells are visible between the developing muscle layers (right) that define the “myogenic zone”. Scale bar=200 μ m. Sections are adjacent to those shown in Figure 2.

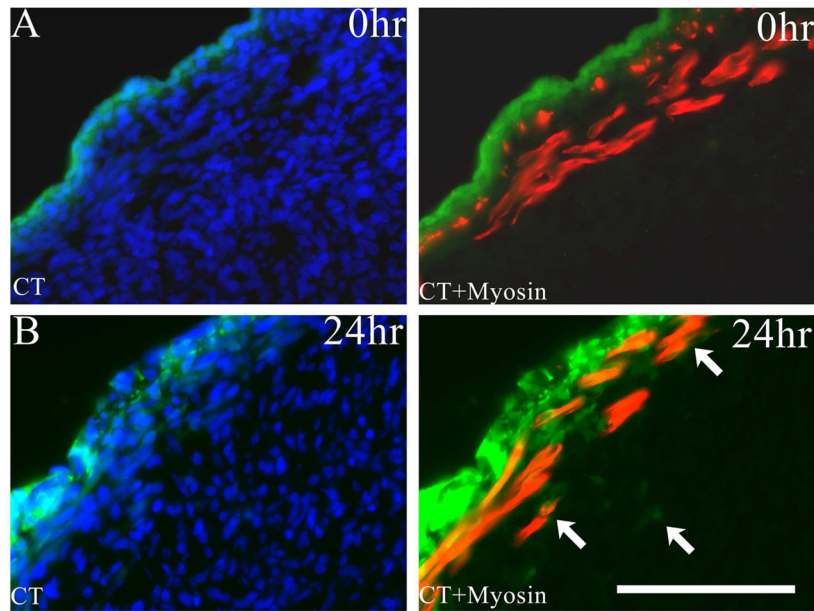


Figure 5.

A. CellTracker™ fluorescent staining (green) of the mesothelial layer after 5-minute exposure of the E17 GCC followed by immediate fixation (0hr). This section shows uptake of the dye by mesothelial cells outside the peripheral muscle layer, which is delineated by myosin heavy chain (MyHC) immunostaining (red). B. Evidence for incorporation of labeled mesothelial cells (green; arrows) within deeper muscle and mesenchymal regions of the GCC after 5-minute CellTracker™ exposure followed by organ culture for 24h. Scale bar=100 μ m.

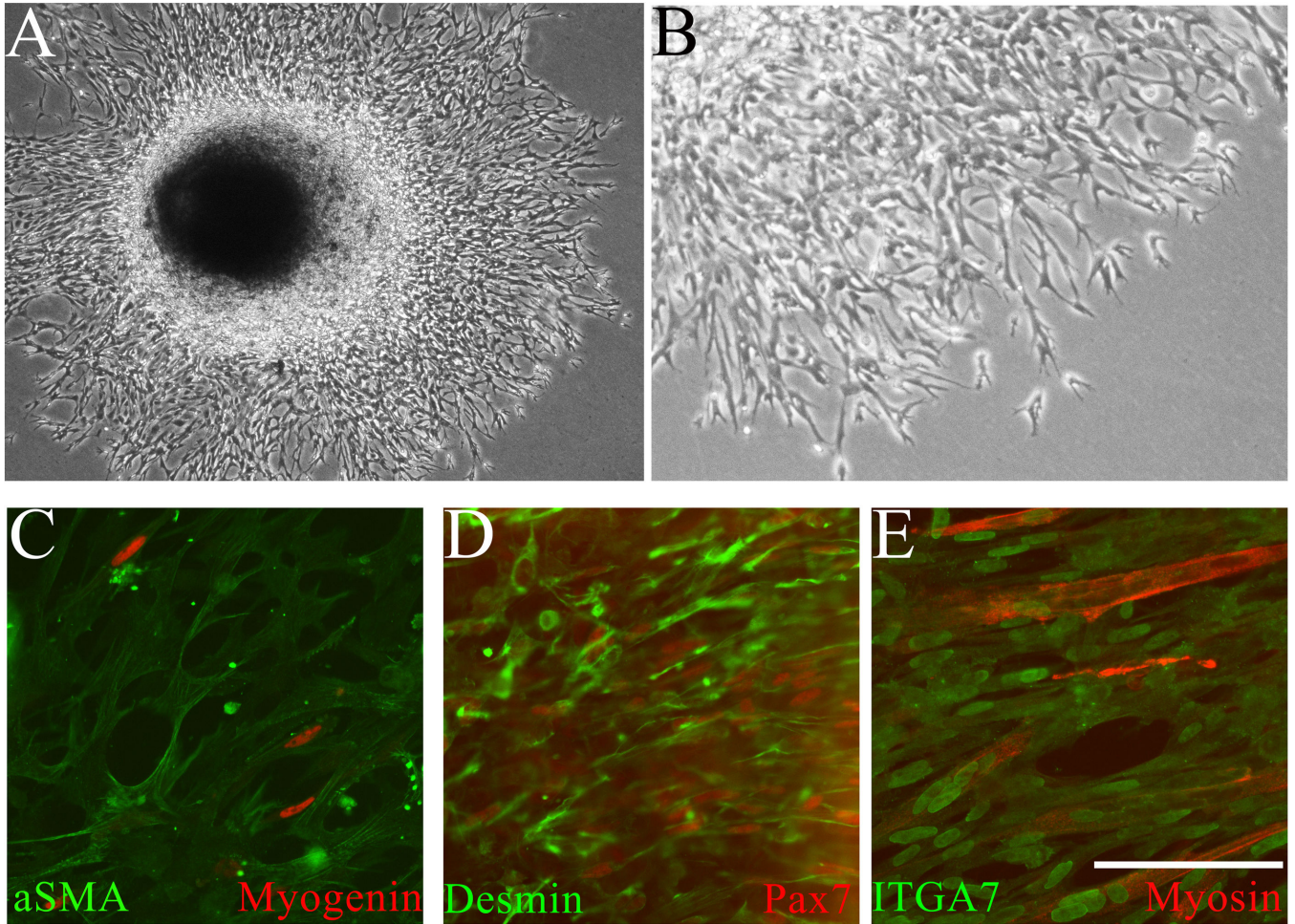


Figure 6.

A. Low- and B. High-power phase contrast images of cultured (3 days) intact E17 GCC grown on poly-L lysine/laminin coated plates and immobilized within Matrigel™. Progressive, peripheral migration of cells was observed throughout the culture period from all borders of the GCC. Higher power image outside the GCC shows an anastomosing cellular architecture. C–E Cells migrating in Matrigel™ were imaged after fixation in situ followed by immunostaining for myogenic markers. C. Ubiquitous expression of smooth muscle alpha actin (α SMA; green) in migrating cells; occasional cells show nuclear localization of myogenin (red). D. All migrating cells express desmin (green); a subset also shows nuclear localization of the myogenic commitment marker paired box 7 (PAX7, red). E. All migrating cells express integrin alpha 7 (ITGA, green) and differentiated muscle is visualized by myosin heavy chain (MyHC, red) expression, showing that some migrating cells form striated myotubes. C–E: scale bar=200 μ m.

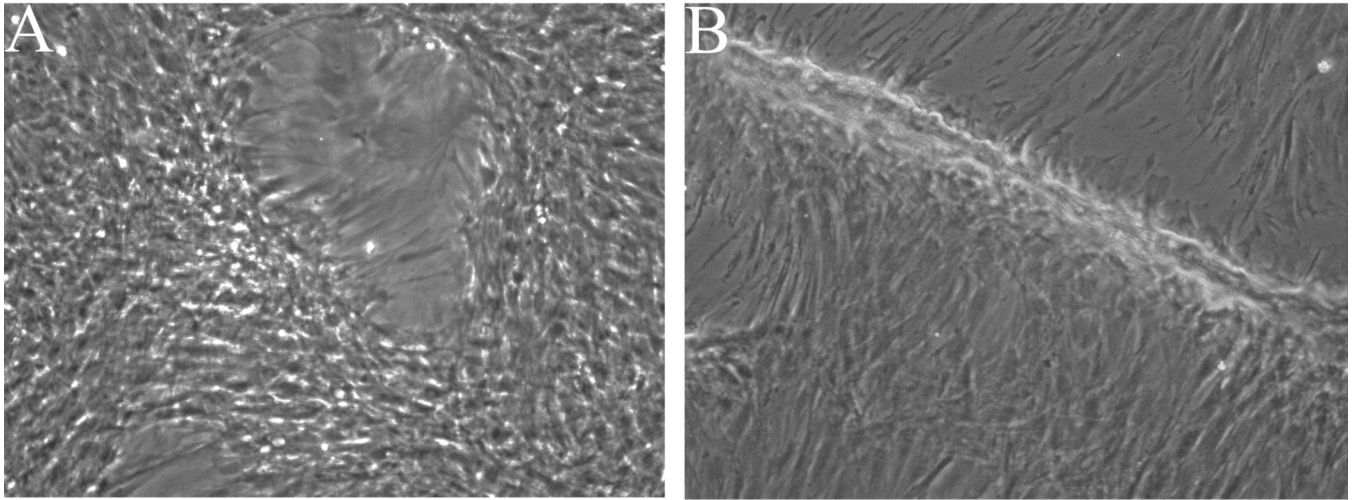


Figure 7. Phase contrast images of passaged (P4 or P6) GCC cells grown to confluence on collagen-I coated plates and visualized after transfer to low serum (2%) medium (20X). **A.** Early appearance of cleared areas created by contraction of the cellular monolayer beginning at day 4 in low serum medium. **B.** More generalized contraction of the cellular monolayer creates elongated, 3D cellular ridges after an additional 5 days of observation together with media changes.

Table 1

Antibodies used in the present study

Protein	Company	ID#	Animal	Concentration	Secondary antibody
Desmin	Abnova	PAB11453	Goat	1:250	DaG488
Myosin heavy chain (MyHC)	DSHB	A4.1025	Mouse	1:50	DaM555
Paired box 7 (Pax7)	DSHB	Pax7	Mouse	1:50	DaM555
Myogenin	DSHB	F5D	Mouse	1:100	DaM555
Smooth muscle alpha actin (α SMA)	Novus	NB600-531	Rabbit	1:250	DaR488
Platelet endothelial cell adhesion molecule (PECAM/CD31)	Novus	NB100-64796	Mouse	1:100	DaM488
Integrin alpha 7 (ITGA7)	Bioss	bs-1816R	Rabbit	1:100	DaR488